J Chim Phys (1995) 92, 205-225

Cluster size effects revisited

J Jortner

School of Chemistry, Tel Aviv University, Ramat Aviv, 69978 Tel Aviv, Israel

Abstract

We address the current 'state of art' of the understanding of cluster size equations, which provide a unified (but not universal) description of the "transition" of energetic, spectroscopic and dynamic attributes of clusters to the infinite bulk system. We explored fundamental issues, e.g., the physical origins of cluster size effects and their dimensionality scaling, and discussed some novel applications for the quantification of the size dependence of site-specific ionization potentials, electronic spectroscopy, collective vibrational excitations and dynamic effects.

Resumé

Nous faisons le point sur les équations concernant les tailles des agrégats qui permettent la description unifiée (mais non universelle) de la "transition" énergétique, spectroscopique et dynamique de ces agrégats vers la phase condensée. Les résultats fondamentaux concernant l'origine physique des effets de taille d'agrégats et de leurs dimensions sont présentés. Quelques applications nouvelles sur la quantification de la dépendance en fonction de la taille des agrégats, des potentiels d'ionisation pour des sites spécifiques, de la spectroscopie électronique, de l'excitation vibrationnelle collective et des effets dynamiques, sont également discutées.

Keywords

Clusters. Size Effects. Electronic Spectroscopy. Collective Vibrational Excitations. Dynamics.

I. Introduction

A key concept for the quantification of the unique characteristics of atomic and molecular clusters[1-18] pertains to size effects.[19-21] These involve the evolution of structural, thermodynamic, electronic, energetic, electromagnetic, dynamic and chemical features of finite systems with increasing the cluster size. Cluster size effects fall into two distinct domains:[19]

(A) Specific size effects. In the "small cluster" size domain an irregular size dependence of the relevant cluster properties $\chi(n)$ (where n is the number of constituents) is exhibited. This irregular pattern is manifested most dramatically in the existence of "magic numbers" in $\chi(n)$ vs n, which reflect shell closure effects. Typical examples involve the structural closed shells of Mackay icosahedra in clusters of rare-gas atoms[22-27] and of spherical large molecules,[28] the enhanced energetic stability and increased ionization potentials for electronic closed shells in metal clusters,[29] and the expected increased stability of the Fermion closed shell structure in $(^3He)_N$ clusters.[30-32]

(B) Smooth size effects, which are revealed for "large" clusters. In this size domain a quantitative

description was advanced[19-21] for the "transition" of energetic, electronic, spectroscopic, electrodynamic and dynamic attributes of clusters to the infinite bulk system in terms of cluster size equations (CSEs),

$$\chi(n) = \chi(\infty) + An^{-\beta} \quad , \tag{1}$$

where A is the constant and β ($\beta \geq 0$) is a positive exponent.

The SCEs specify the "critical" cluster size for which a specific property becomes size invariant and does not differ in any significant way from that of a macroscopic sample of that material. From the foregoing analysis of cluster size effects[19-21] it became apparent that the "critical" cluster size for which the properties of bulk matter are reached, depends on the nature of the experimental observable. The CSEs in their applicability range constitute a "theory of everything"[19] regarding the properties of (large) clusters, providing a unified (but not universal) description of the merging between the properties of microscopic large finite systems and those of a macroscopic bulk material. Since the advance of the underlying concepts and the unified description of CSEs,[19] considerable progress has been made on several fronts of cluster chemical physics, which pertain to

(1) The elucidation of the physical origins of cluster size effects, which originate either from cluster packing or from excluded volume effects.[21]

(2) The formulation of dimensionality scaling of cluster size effects.[21,33]

(3) The presentation of CSEs for central, surface, and site-specific configuration of an impurity atom or molecule in heteroclusters and in neat clusters.[34]

(4) Some new applications of CSEs to the electronic spectroscopy of clusters.[20,33]

(5) The formulation and application of CSEs to collective vibrational excitations of clusters.[21]

(6) The advance of dynamic CSEs for a new field of cluster-wall collisions.[35,36]

These novel and basic features of cluster size effects constitute the subject matter of this article.

II. Origins of Cluster Size Effects

CSEs, which are quantified by Eq. (1), can be traced to two distinct physical origins: cluster packing and excluded volume effects. These two categories will now be considered.

(II.A) Size effects originating from cluster packing.

These effects pertain to the consequences of the large surface/volume fraction of clusters. For sufficiently large clusters, the fraction of the surface atoms is[19,37,38]

$$F = \alpha n^{-1/3} \quad , \tag{2}$$

where α is a numerical constant, which is determined by the cluster shape (i.e., $\alpha = 4$ for a sphere).

A straightforward utilization of this result pertains to the description of extensive variables Y, e.g., the internal energy, entropy or magnetization, of the cluster. Viewing the cluster of n constituents as a composite system consisting of surface and volume subsystems, the value of the extensive variable Y(n) is obtained from an additivity rule for these subsystems

$$Y(n) = n(1-F)y_v + nFy_s \ , \tag{3}$$

where y_v and y_s are the corresponding variables (per constituent) for the bulk and for the surface, respectively. The total value of the variable per constituent $y(n) = Y(n)/n$ is obtained from Eqs. (2) and (3) in the form

$$y(n) = y_v + \alpha(y_s - y_v)n^{-1/3} \ . \tag{4}$$

Eqs. (2) and (4) constitute simple applications of the liquid drop model,[37,38] which was advanced in nuclear physics. Eq. (4) is isomorphous to the CSE, Eq. (1).

A useful application of the CSE, Eq. (4), due to cluster packing, involves the description of the internal energy per constituent $u(n) = U(n)/n$ of the cluster of total internal energy n, which can be described in the form

$$u(n) = u_v + \alpha(u_s - u_v)n^{-1/3} \ , \tag{5}$$

where u_v and u_s are the energy (per constituent) for the volume and surface constituents, respectively. As is apparent from Fig. 12 of reference 19, the CSE, Eq. (5), accounts well for the cohesion energy of Na_n clusters, with u(n) vs n conversing to the asymptotic value $u(\infty) = u_v$, which corresponds to the bulk heat of sublimation. The CSE parameters are $u_v = -1.12$ eV and $\alpha(u_s - u_v) = 1.05$ eV for Na_n and $u_v = -0.94$ eV and $\alpha(u_s - u_v) = 0.96$ eV for K_n.[39,40] The values of u_v indeed coincide with the bulk cohesive energies. Taking $\alpha = 4$ we estimate for the surface energies $u_s = -0.86$ eV for Na_n and $u_s = -0.70$ eV for K_n, with the values of the volume and surface constituent energies being $|u_v| > |u_s|$ for both families of clusters.

(II.B) Size effects originating from excluded volume contributions.

A multitude of energetic and spectroscopic size effects can be described in terms of the infinite system observable, which is corrected to the excluded volume contribution. The CSE, Eq. (1), then assumes the general form

$$\chi(n) = \chi(\infty) + C(n) \ , \tag{6}$$

where

$$C(n) = An^{-\beta} \tag{7}$$

is the excluded volume correction term. C(n) accounts for the modification of the bulk value for the observable in the cluster, due to the excluded volume outside it (i.e., the range R_c to ∞). R_c is the cluster radius, which is related to the radius R_0 of a single constituent by

$$R_c = R_0 n^{1/3} \ . \tag{8}$$

Accordingly, the excluded volume correction can be expressed in the alternative form

$$C(R_c) = A(R_c/R_0)^{-3\beta} \ . \tag{9}$$

As was previously pointed out,[19] the CSE, Eq. (6), is better than it appears at first sight for the quantification of the physical observables. All the short-range contributions to $\chi(n)$, which are usually difficult to evaluate, are incorporated in $\chi(\infty)$, which is often taken from experiment. What is explicitly evaluated is the correction term C(n) arising from the excluded volume contributions. These excluded volume contributions are determined by long-range effects, which are amenable to a reliable calculation. We shall now apply excluded volume effects to the energetics of clusters, while spectroscopic size effects will be explored in section IV.

III. Excluded Volume Effects on Cluster Ionization Energetics

The CSE, due to excluded volume effects, was successfully applied to the energetics of ionization of elemental, metallic and ionic clusters. Here C(n), Eqs. (7) or (9), originates from the charging energy contributions to the cluster ionization potential. The application of the continuum dielectric model for the excluded volume outside the cluster results in $C(R_c) \propto R_c^{-1}$, so that C(n) is given by Eq. (7) with $\beta = 1/3$. This situation is realized for the vertical ionization potentials of rare-gas clusters,[19] the ionization potentials of metal clusters[19] and the vertical binding energies of interior excess electron states in large $(NH_3)_n^-$ clusters.[19,41]

Three extensions of the CSEs, which originate from excluded volume effects are of interest:

(III.A) Self volume corrections for an impurity in heteroclusters.

Such an impurity, e.g., an atom, molecule or ion, acts as a probe for the cluster energetics and dynamics. The ionization potential of an impurity solvated in the center of a cluster, which is described in terms of a continuum dielectric model, results in the modification of the excluded volume contribution, Eq. (7), to[34,36,42,43]

$$C(n) = A(n+\xi)^{-\beta} \quad , \tag{10}$$

with $\beta = 1/3$, where ξ represents the self-volume of the impurity relative to the other cluster constituents. This self-volume correction was recently applied for the analysis of the vertical ionization potentials of solvated anion clusters.

(III.B) Ionization potentials of surface and interior impurity states.

The excluded volume charging energy contribution to the ionization potential of a cluster containing an impurity, e.g., an atom, a molecule or an ion, depends on the location of the impurity within the cluster. The distinction between the surface and the interior impurity configuration is of considerable interest in the context of anion solvation in water clusters, e.g., $X^-(H_2O)_n$ (X = F, Cℓ, Br, I)[34,42,43-55] and of rare gas heteroclusters, e.g., $XeAr_n$.[56-60] The difference between the CSE for interior and surface states is manifested both in the form of the excluded volume correction, Eq. (7) and in the corresponding bulk value. As an instructive example consider the ionization potential of large $XeAr_n$ clusters, treated by a dielectric model.[34,61-64] A justification for the application of the dielectric model for the ionization potential of sufficiently large clusters (i.e., $R_c >> R_{IM}$, where R_{IM} is the impurity radius) is provided by the analysis of the energetics of ionization of an impurity in bulk rare gases,[65] which incorporates two-body and three-body interactions. The dielectric model for the ionization potential of a neutral heterocluster e.g., $XeAr_n$, gives

$$IP(R_c) = IP(\infty) + C(R_c) \quad . \tag{11}$$

For the Xe atom being located in the center of the cluster we have[19]

$$IP^{(c)}(\infty) = IP_g - (e^2/2R_{IM})(1-1/\in) \quad , \tag{12a}$$

$$C^{(c)}(R_c) = (e^2/2R_c)(1-1/\in) \quad , \tag{12b}$$

where IP_g is the impurity gas phase ionization potential and $\in$ is the (optical) dielectric constant of the exterior excluded volume of the nonpolar material. For the surface configuration, with the Xe atom being located inside the cluster surface at the distance $r = R_c - R_{IM}$ from the center, the application of the dielectric model[34,61-63] to the size dependent ionization potential results in

$$IP(R_c) = IP_g - (e^2/2R_{IM})(1-1/\in) + (e^2/2R_c) \sum_{j=0}^{\infty} f_j(\in) [(R_c - R_{IM})/R_c]^{2j} \quad , \tag{13}$$

where

$$f_j(\epsilon) = (\epsilon-1)(j+1)/\epsilon(j\epsilon+j+1) \quad . \tag{14}$$

Eq. (13) results in the following contributions, Eq. (11), to the inside-surface CSE,

$$IP^{(is)}(\infty) = IP_g - (e^2/2R_{IM})(1-1/\epsilon)[1-1/2(\epsilon+1)] \quad , \tag{15a}$$

and

$$C^{(is)}(R_c) = (e^2/2R_c) \sum_{j=0}^{\infty} f_j(\epsilon) [(R_c-R_{IM})/R_c]^{2j} + g(\infty) \quad , \tag{15b}$$

where

$$g(\infty) = IP^{(c)}(\infty) - IP^{(is)}(\infty) \quad . \tag{16}$$

We note that the ionization potential of the neutral impurity atom inside the macrosurface of a nonpolar medium, Eq. (15a), is higher than that of an interior state, Eq. (12a), i.e., $g(\infty) < 0$, as expected. This feature of the surface state of a neutral impurity in a nonpolar medium (i.e., $\epsilon = \epsilon_s \simeq \epsilon_\infty$, where ϵ_∞ and ϵ_s are the optical and static dielectric constants, respectively) is distinct from that of a polar cluster ($\epsilon_s > \epsilon_\infty$).[34] One can readily apply the analysis of Cheshnovsky, Giniger, Markovich, Makov, Nitzan and Jortner,[34] which was developed to account for the size dependence of the vertical ionization potential to anion-water clusters. For a neutral impurity in a central configuration in a polar cluster

$$IP^{(c)}(\infty) = IP_g - (e^2/2R_{IM}) [1-2/\epsilon_s+1/\epsilon_\infty] \tag{17a}$$

and

$$C^{(c)}(R_c) = (e^2/2R_c)[1-2/\epsilon_s+1/\epsilon_\infty] \, , \tag{17b}$$

while for the interior surface configuration[34]

$$IP^{(is)}(\infty) = IP^{(c)}(\infty)-(e^2/4R_{IM}) \left[\frac{(\epsilon_\infty-1)}{\epsilon_\infty(\epsilon_\infty+1)} - 2 \, \frac{(\epsilon_s-1)}{\epsilon_s(\epsilon_s+1)} \right] \tag{18a}$$

and

$$C^{(is)}(R_c) = (e^2/2R_c) \sum_{j=0}^{\infty} [2f_j(\epsilon_s)-f_j(\epsilon_\infty)] [(R_c-R_{IM})/R_c]^{2j} + g(\infty) \quad . \tag{18b}$$

The above applies for clusters of polar molecules with $\epsilon_s >> \epsilon_\infty$, where we have $g(\infty) > 0$, exhibiting the reduction of the neutral impurity ionization potential at the macrosurface relative to the bulk value.

This counterintuitive reduction effect in a polar medium was traced by Chesnovsky et al[34] to the surface enhancement of repulsive interactions involving induced dipoles. Cheshnovsky et al[34] applied the dielectric model to the size dependence surface ionization potentials of negative ions and on surface configurations of the negative anion in water clusters.

(III.C) Site-specific ionization potentials of clusters.

The ionization potentials of distinct sites in a neat elemental or molecular cluster are different. The same applies to different substitutional sites of an impurity in heteroclusters. The application of the dielectric model[34,61-63] to the ionization of a neutral constituent or an impurity located at the distance r from the center of a polar ($\epsilon_s > \epsilon_\infty$) or nonpolar ($\epsilon_s = \epsilon_\infty$) cluster, results in

$$IP(r,R_c) = IP_g - (e^2/2R_{IM})(1-2/\epsilon_s+1/\epsilon_\infty) + (e^2/2R_c)(1-2/\epsilon_s+1/\epsilon_\infty) + \\ + (e^2/2R_c)\sum_{j=1}^{\infty}[2f_j(\epsilon_s)-f_j(\epsilon_\infty)](r/R_c)^{2j} \quad . \tag{19}$$

The second term of the RHS of Eq. (19) constitutes $C^{(c)}(R_c)$, Eq. (17b), while the third term provides the site-specific correction to the central site cluster ionization potential. The site dependence of the ionization potential is manifested by the r dependence of $IP(r,R_c)$, which is due to the third term on the RHS of Eq. (19). We note in passing that Eq. (19) was presented for the site-specific ionization of an impurity of radius R_{IM}. The same relation is applicable for the ionization of a specific constituent (at distance r) of a neat cluster with R_{IM} being replaced by R_0. Model calculations reveal that the r dependence of $IP(r,R_c)$ is weak in the cluster interior, i.e., $r/R \leq 0.8$, so that very accurate ionization potential data are required to distinguish between different interior locations within the cluster (e.g., atomic shell structure in the interior of rigid rare gas clusters). On the other hand, in the vicinity of the cluster surface (i.e., $r/R > 0.8$), a marked sensitivity of $IP(r,R)$ on the location of the ionized site is exhibited, allowing for the interrogation of different surface configurations in nonpolar and in polar clusters.

Eq. (19) provides the result for site-specific ionization potentials of the cluster. Energy resolved studies of the ionization potential of a mass-selected rigid cluster will result in an inhomogeneous distribution of $IP(r,R_c)$, Eq. (19), whose values are weighed by the abundance of the sites. The averaged ionization potential of an ensemble of mass-selected neat clusters will be given by an average over the different sites. Making use of Eqs. (17) and (19) one gets the configurational averaged value

$$\langle IP(R_c)\rangle = \int dr\, P(r) IP(r,R_c) = IP^{(c)}(\infty) + C^{(c)}(R_c) + \\ (e^2/2R_c)\int_0^{R_c} dr P(r) \sum_{j=1}^{\infty}[2f_j(\epsilon_s)-f_j(\epsilon_\infty)](r/R_c)^{2j} \quad , \tag{20}$$

where P(r) is the site r population probability. For neat clusters P(r) is taken as a simple homogeneous distribution, i.e., $P(r) = 3r^2/R_c^3$, resulting in in the configurationally averaged ionization potential

$$\langle IP(R_c)\rangle = IP^{(c)}(\infty) + C^{(c)}(R_c) + (e^2/2R_c) \sum_{j=1}^{\infty} [3/(2j+3)]\,[2f_j(\epsilon_s)-f_j(\epsilon_\infty)] \tag{21}$$

Eq. (21) is of the form of a CSE

$$\langle IP(R_c)\rangle = IP^{(c)}(\infty) + \langle C(R_c)\rangle \ , \tag{22}$$

with the excluded volume correction being

$$\langle C(R_c)\rangle = C^{(c)}(R_c) + (e^2/2R_c) \sum_{j=1}^{\infty} [3/(2j+3)][2f_j(\epsilon_s)-f_j(\epsilon_\infty)] \ , \tag{23}$$

which assumes the conventional form $\langle C(R_c)\rangle \propto R_c^{-1} \propto n^{-1/3}$. Finally, we can consider the ensemble average of mass-selected heteroclusters each containing an impurity atom. The averaged ionization potential is again given by Eq. (20), with P(r) representing the probability of the site population, which is determined by the cluster preparation conditions.

This analysis of sections (III.B) and (III.C) extends the previous simple picture[19] of the cluster size dependence of ionization potentials to incorporate site specific effects and to provide a distinction between interior configurations. The electronic spectroscopy of extravalence excitations of Xe in $XeAr_n$ was studied by Möller et al.[56-59] These significant studies,[56-59] in conjunction with simulations of the optical lineshapes,[60] provided extensive information on site-specific electronic excitations. The explorations of site-specific ionization potentials will be of considerable interest. These $XeAr_n$ clusters provide a generic example for elemental heteroclusters. We now proceed to explore the spectroscopy of more complex heteroclusters.

IV. Excluded Volume Effects on Heterocluster Spectroscopy

Optical absorption spectra of $M{\cdot}A_n$ heteroclusters, consisting of an aromatic molecule (M) embedded in a cluster of inert-gas atoms (A) which correspond to an intravalence excitation of M, are of interest in relation to the microscopic interrogation of solvation phenomena and for the utilization of M as a probe for the cluster microenvironment and nuclear dynamics.[66-88] The cluster size dependence of the electronic excitations, i.e., the spectral lineshapes, their spectral shifts $\delta\nu$ and their second central moments Δ, can be quantified in terms of CSEs.[20,33] The CSEs for the optical properties rest on a spherical representation of the cluster with the impurity being located in an interior configuration at the center of the cluster. The spectral shifts are due to cumulative M-A dispersive interactions, while

the second moment originates from short-range nuclear dynamic effects.[20] The spectral shift is $\delta\nu = M_1$, where M_1 is the first moment of the absorption band. The evaluation of M_1 results in the spectral shift[20]

$$\delta\nu = \bar{\rho} \int_0^{R_c} d^3\underset{\sim}{r}\; e(\underset{\sim}{r})\, g(\underset{\sim}{r}) \quad , \tag{24}$$

where $\bar{\rho}$ is the average density, $g(\underset{\sim}{r})$ represents the isotropic radial distribution function and $e(\underset{\sim}{r})$ corresponds to the microscopic (dispersive) spectral shift exerted on M by a single atom located at $\underset{\sim}{r}$. The central second moment of the spectral lineshape $\Delta = (M_2 - M_1^2)^{1/2}$, where M_2 is the second moment of the band, is given in the form[20]

$$\Delta(R_c) = \bar{\xi}^{1/2} \left[\int_0^{R_c} d^3\underset{\sim}{r}\; [e(\underset{\sim}{r}) g(\underset{\sim}{r})]^2 \right]^{1/2} \quad . \tag{25}$$

$\bar{\xi} = \bar{\rho}^2 k_B T \kappa_T$, where κ_T is the isothermal compressibility, taken for a bulk material.

In the slow modulation limit in the stochastic model for the absorption lineshapes,[33,60,77,89-91] i.e., $\tau_c \Delta/\hbar < 1$, where τ_c is the correlation time for the decay of the autocorrelation function of the energy gap, the homogeneous linewidth is

$$\Gamma_s \simeq \eta\Delta \quad , \tag{26}$$

where $\eta = 2.355$. In the fast modulation limit, i.e., $\tau_c \Delta/\hbar << 1$, the linewidth is

$$\Gamma_f = 2\Delta^2 \tau_c/\hbar \quad . \tag{27}$$

Eqs. (26) and (27) relate the central second moment to the homogeneous linewidth.

The spectroscopic observables, Eqs. (24) and (25), are determined by integrals of the powers of the product $e(\underset{\sim}{r})g(\underset{\sim}{r})$ over the cluster volume. This cluster size dependence provides the basis for the CSEs for $\delta\nu(R_c)$ and $\Delta(R_c)$. We express the two lowest spectral moments $M_1(R_c)$ and $[\Delta(R_c)]^2$ of the cluster in terms of the moments $M_1(\infty)$ and $[\Delta(\infty)]^2$ of the bulk system, which are corrected to the contribution of the excluded volume, i.e.,

$$M_1(R_c) = M_1(\infty) - C_1(R_c) \tag{28a}$$

and

$$[\Delta(R_c)]^2 = [\Delta(\infty)]^2 - C_2(R_c) \quad , \tag{28b}$$

where the excluded volume corrections are

$$C_1(R_c) = \bar{\rho} \int_{R_c}^{\infty} d^3\vec{r}\, e(\vec{r})\, g(\vec{r}) \tag{29a}$$

$$C_2(R_c) = \bar{\xi} \int_{R_c}^{\infty} d^3\vec{r}\, [e(\vec{r})g(\vec{r})]^2 \quad . \tag{29b}$$

As usual, we consider a sufficiently large cluster (with $R_c >> R_M > R_0$, where R_M is the average radius of M), where the excluded volume ($r \geq R_c$) is microscopically homogeneous, i.e., $g(\vec{r}) = 1$. The microscopic dispersive spectral shifts exerted by the atoms in the excluded region can be taken as isotopic in their asymptotic form

$$e(r) = -\gamma/r^6 \quad . \tag{30}$$

Eqs. (28) and (29) for an $M{\cdot}A_n$ heterocluster then result in the correction to M_1: $C_1(R_c) = \bar{A}_1 R_c^{-3} = A_1 n^{-1}$, where $\bar{A}_1 = -4\pi\gamma\bar{\rho}/3 = -\gamma R_0^{-3}$ and $A_1 = -\gamma/R_0^6$. For the correction to Δ we get $C_2(R_c) = \bar{A}_2 R_c^{-9} = A_2 n^{-3}$, where $\bar{A}_2 = 4\pi\bar{\xi}\gamma^2/9$ and $A_2 = 4\pi\bar{\xi}\gamma^2/9R_0^9$.

The CSEs for the experimental observables are now obtained by applying the excluded volume corrections to Eqs. (24) and (25), resulting in the spectral shift

$$\delta\nu(n) = \delta\nu(\infty) + A\, n^{-1} \quad , \tag{31}$$

where $A = A_1 = \gamma/R_0^6$.

The linewidths are determined by Δ, which exhibits the size dependence

$$\Delta(n) = \Delta(\infty) - \bar{B}n^{-3} \quad , \tag{32}$$

where $\bar{B} = A_2/2\Delta(\infty)$. The spectral linewidth in the fast modulation limit is

$$\Gamma_f(n) = \Gamma_f(\infty) - (2A_2\tau_c/\hbar)n^{-3} \quad , \tag{33}$$

while for the slow modulation limit

$$\Gamma_s(n) = \Gamma_s(\infty) - Bn^{-3} \quad , \tag{34}$$

where $B = A_2/2\Delta(\infty)$. Eq. (33) for homogeneous broadening (dephasing) under fast modulation

contains τ_c, whose size dependence is unknown. Eq. (33) for slow modulation is useful for large clusters, with the parameter B appearing in this limit being

$$B = (k_B T \kappa_T / 8\pi R_0^3 \Delta(\infty)) \quad . \tag{35}$$

Eqs. (31) and (35) establish a relation between the excluded volume corrections to the two spectroscopic observables with

$$B = (\eta^2 / 8\pi \Gamma_s(\infty)) \, (k_B T \, \kappa_T / R_0^3) \, A^2 \quad . \tag{36}$$

The CSEs for $\delta\nu(n)$ and for $\Delta(n)$, i.e., $\Gamma_s(n)$ and $\Gamma_f(n)$, imply that the size dependence of the two spectroscopic observables is different, providing another specific example for the nonuniversality of the CSEs. $\beta = -1$ for $\delta\nu(n)$ represents the cumulative contribution of the dispersive microscopic shifts, Eq. (30), while $\beta = -3$ for $\Delta(n)$ originates from the effects of density fluctuations on the dispersive interactions. With increasing the heterocluster size, the spectral shifts are expected to converge gradually (as $|\delta\nu(n) - \delta\nu(\infty)| \propto n^{-1}$) to the bulk value, whereas in the $M \cdot A_n$ heterocluster size domain n = 10-100 the bulk value was not yet achieved. On the other hand, the homogeneous linewidths converge fast (as $|\Delta(n) - \Delta(\infty)| \propto n^{-3}$) to their bulk value and near saturation is expected to be achieved already for $n \geq 10$.

The test of the CSEs, Eqs. (31) and (34), is provided by experimental data[75] and MD simulations[75] for $\delta\nu(n)$ and by MD simulations for 9,10 dichloroanthracene (DCA)-inert gas heteroclusters. In Fig. 1 we portray the size dependence of $\delta\nu(n)$ and $\Gamma_s(n)$ for $DCA \cdot Kr_n$ (n = 5-28) heteroclusters. The increase of $|\delta\nu(n)|$ with increasing n is well accounted for by Eq. (31), while the weak size dependence of $\Gamma_s(n)$ is qualitatively consistent with the predictions of Eq. (33).

To provide a quantification of the spectroscopic CSEs we present in Fig. 2 the experimental data for the size dependence of the spectral shifts of $DCA \cdot Ar_n$ (n = 1-55) heteroclusters, together with the results of MD simulations of this observable,[75] which are in excellent agreement with the experimental data. In the size domain n = 30-55, $\delta\nu(n)$ exhibits a monotonous, though pronounced, size dependence which is consistent with Eq. (31) with $\delta\nu(\infty) = -610$ cm^{-1}. In the insert to Fig. 2 we analyze the available experimental data for the cluster size dependence of $\delta\nu(n)$ for $DCA \cdot Ar_n$, with n = 30-55,[75] for n = 1000±500 [92] and for $n = \infty$,[93] (i.e., the Ar matrix spectrum). These experimental data follow the linear relationship

$$\delta\nu(n)/\text{cm}^{-1} = -610 + 4.2 \times 10^3 \, n^{-1} \quad .$$

As expected from Eq. (31) the functional form of the CSE for $\delta\nu(n)$ is obeyed with the appropriate parameters: (i) The intercept $\delta\nu(\infty) = -610$ cm^{-1} coincides with the experimental value of $\delta\nu(\infty)$ for DCA in the Ar matrix;[93] (ii) The slope A of this CSE is expected to be given by Eq. (31). From the calculation of the asymptotic behavior of the microscopic spectral shifts at a large M-A

distance for DCA-Ar or anthracene-Ar, Eq. (30) is obeyed with $\beta = 2.0\times10^5$ cm^{-1} Å^6, which, together with $R_0 = 2.08$ Å for the Ar cluster medium, results in $A = \beta/R_0^6 = 2.7\times10^3$ cm^{-1}. This calculated value of A is in reasonable agreement with the experimental value $A = 4.2\times10^3$ cm^{-1}. Next, we proceed to the evaluation of the parameter B, which determines the CSE for $\Delta(n)$, Eq. (31), for $DCA\cdot Ar_n$ heteroclusters. To calculate B, Eqs. (29a) and (35), we utilize the Ar bulk data (for solid Ar)[94] $\kappa_T = 2.0\times10^{-9}$m^{2}N^{-1} and $R_0 = 2.08\times10^{-10}$m, which, together with T = 10K, $\eta = 2.355$, the simulated data $\Gamma_s(\infty) = 35$ cm^{-1} at 20K and the experimental result (Fig. 2) $A = 4.2\times10^3$ cm^{-1}, results in $B = 40$ cm^{-1}. Thus the heterocluster size dependence of $\Gamma_s(n)$ is expected to saturate for a very small heterocluster size, in accord with the results of the MD simulations (Fig. 1) of the weak cluster size dependence of $\Delta(n)$. This analysis of the spectroscopy and of the ionization energetics (section III) concludes our discussion of excluded volume effects. We now proceed to explore the implications of cluster packing on dynamic effects.

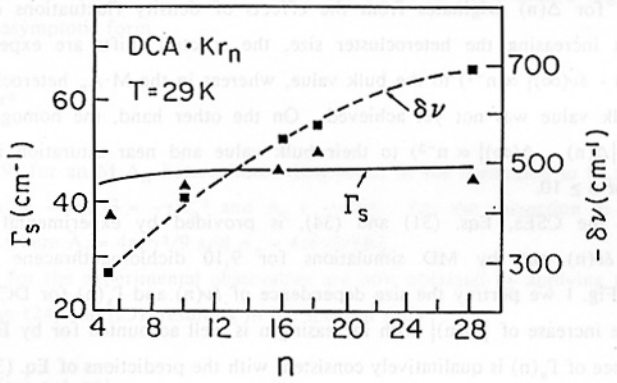

Fig. 1 MD simulations of the spectral shifts $\delta\nu$ (■) and of the homogeneous linewidths, $\Gamma_s = \eta\Delta$ (Δ) for the large $DCA\cdot Kr_n$ (n = 5-28) clusters at 29 K according to Ref. 75. The simulation results were fit by the CSEs for these observables. The dashed line represents the CSE for $\delta\nu$, Eq. (31), with $\delta\nu(\infty) = -900$ cm^{-1} and $A = 5.6\cdot10^3$ cm^{-1}. The solid line represents the CSE for Δ, Eq. (34), with $\Delta(\infty) = 45$ cm^{-1} and $B = 40$ cm^{-1}

V. Bulk and Surface Collective Vibrational Modes

An interesting example of size effects, originating from cluster packing, are surface collective vibrational modes and interior compression modes.[37,38] The collective cluster excitations can be treated by the application of the nuclear physics liquid drop model.[37,38] The frequencies of surface collective modes are

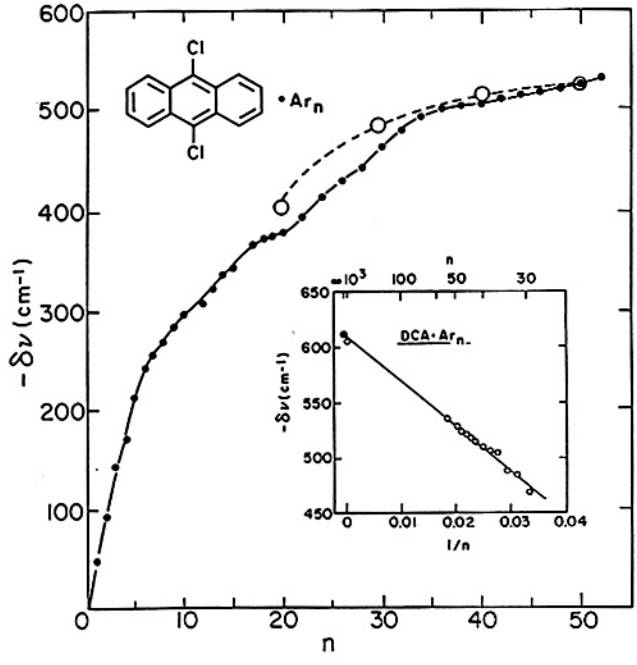

Fig. 2. The size dependence of the experimental $\delta\nu$ data for DCA·Ar$_n$ (n = 1-55) clusters from Ref. 75 (• and solid curve). For large clusters $\delta\nu$ is accounted for by the CSE, Eq. (31), presented by open circles (O and dashed curve). The insert shows the CSE for these experimental $\delta\nu$ data for n = 30-55 (Ref. 75), n = 1000±500 (Ref. 92) and the bulk solid (Ref. 93), which display the linear relation of $\delta\nu$ vs n^{-1}, according to Eq. (31).

$$\hbar\omega_s(n) = an^{-1/2} \quad , \tag{37}$$

where $a = [\ell(\ell-1)(\ell+2)A_s/3\mu R_0^2]$. Here ℓ is the angular momentum quantum number, A_s the surface energy, i.e., $A_s = |\alpha(u_s - u_v)|$, according to Eq. (5), and R_0 is the radius of a single constituent of mass μ. The frequency of the interior mode of compression breathing is

$$\hbar\omega_b(n) = bn^{-1/3} \quad , \tag{38}$$

where $b = \gamma\hbar c/R_0$ and c is the velocity of sound. The distinct size dependence of $\hbar\omega_s(n)$ and $\hbar\omega_b(n)$ originates from the different dispersion laws for surface riplons ($\omega(q) \propto q^{3/2}$) and for bulk compression excitations ($\Omega(q) \propto q$). Note that for these vibrational modes for the liquid (nonrigid) cluster $\hbar\omega_s(\infty) = \hbar\omega_b(\infty) = 0$. For a rigid (solid) cluster the interior compression mode, Eq. (38), has to be modified to

include the contribution $\hbar\omega_b(\infty)$ of the surface phonons of the infinite solid, resulting in the CSE

$$\hbar\omega_b(n) = \hbar\omega_b(\infty) + bn^{-1/3} \quad . \tag{39}$$

Vibrational collective excitations of $(^4He)_n$ and $(^3He)_n$ clusters, which are liquid down to 0 K [96] were calculated[95,96] resulting in $\hbar\omega_b(n) = 25.6n^{-1/3}$ K for $(^4He)_n$ (Fig. 3) and $\hbar\omega_b(n) = 17.9n^{-1/3}$ K for $(^3He)_N$ (Fig. 4). For the quadrupole ($\ell = 2$) surface modes of $(^4He)_n$ the collective vibrational excitations are $\hbar\omega_s(n) = 10.5n^{-1/2}$ K (Fig. 3).

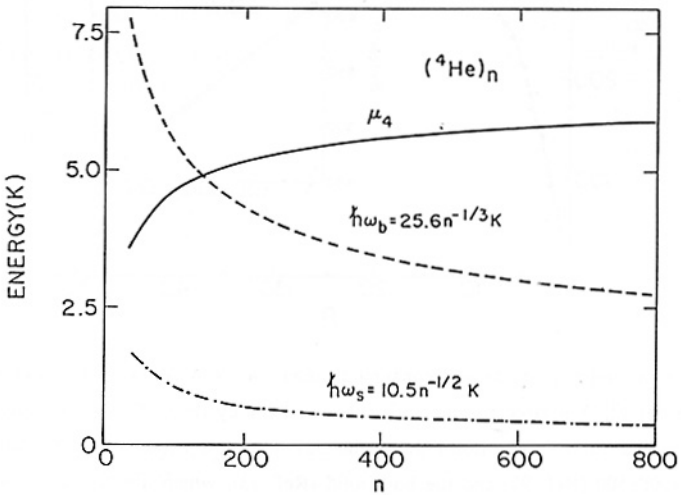

Fig. 3. Cluster size dependence of the energies of the surface ($\hbar\omega_s$) and interior compression ($\hbar\omega_b$) collective vibrational modes of $(^4He)_n$ clusters. The CSEs, Eqs. (37) and (38), were used for the calculation. μ_4 is the binding energy per atom.

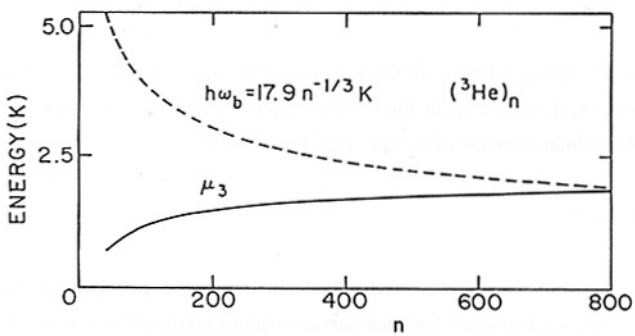

Fig. 4. Cluster size dependence of the energy of the interior compression collective vibrational mode of $(^3He)_n$ clusters, as calculated from Eq. (38). μ_3 is the binding energy per atom.

No direct experimental observations of these collective vibrational excitations for $(He)_n$ clusters are yet available. On the experimental front, some interesting expectations can be provided. The binding energies per atom μ_4 for $(^4He)_n$ and μ_3 for $(^3He)_n$ are smaller than the frequency of the interior mode for relatively small clusters, i.e., $\mu_4 < \hbar\omega_b(n)$ for $n < 180$ and $\mu_3 < \hbar\omega_b(n)$ for $n < 800$ (Figures 3 and 4). In this cluster size domain one-quantum induced evaporation of ^4He or ^3He atoms from the luster will occur. The size onset for this single atom evaporation will exhibit a striking isotope effect. The quadrupole surface collective vibrational frequencies are too low relative to μ_4 (Fig. 3) to induce a one-quantum evaporation. A more isoteric implication of these collective vibrational modes pertains to their coupling to electronic states of an excess electron on the surface of a large $(He)_n$ cluster.[97-100] These bound surface excess electron states[97-100] constitute giant electronic states with weak (ground state) binding energies, $E_{1,0}$, i.e.,[100] $-0.695\ meV \leq E_{1,0} \leq 0$, which raise interesting questions regarding the separation of electronic and nuclear motion in these systems. For large clusters in the size domain $n \simeq 10^6$, $E_{10} \simeq -0.26$ K and the electronic energy is comparable to the vibrational interior collective mode ($\hbar\omega_b \simeq 0.26$ K). Under these extraordinary circumstances the conventional Born-Oppenheimer separability between electronic and nuclear motion may break down.[100]

A beautiful experimental verification of the existence of the cluster compression breathing mode was obtained by Buck and Krohne[101] from scattering of He atoms from Ar_n ($n = 25$-4600) clusters. The cluster size dependence of the maximum of the vibrational energy transfer obeys the CSE, Eq. (39), with the intercept $\hbar\omega_b(\infty)$ being given by the Rayleigh mode of the (001) surface phonons of bulk solid Ar.

VI. Dynamic Cluster Size Effects

High-energy cluster-wall collisions[35,36,102-126] (with the acceleration of atomic or molecular cluster ions containing 10-500 constituents to velocities up to $v \sim 50$ kmsec^{-1} and kinetic energies up to $E_v \sim 100$ KeV) involve a novel high-energy, ultrafast, cluster size dependent energy acquisition process.[35,103,104,126] When an internally cold, but rapidly moving, cluster collides with a relatively incompressible solid surface, a microscopic shock wave with an extremely high transient particle density (~ 4 fold of the standard density), temperature (up to 10^6 K) and energy density (up to ~ 100 eV/particle) can be temporarily generated within the cluster on the fsec time scale, which constitutes a new medium, in which novel processes of energy acquisition and disposal are expected to occur. During the ultrashort time domain of the cluster-wall collision, thermal equilibrium is not approached, but rather energy may be localized, resulting in pair energies considerably exceeding the equilibrium energy.[35,36]

The energy acquisition process for cluster-wall high-energy collision can be characterized by the residence time τ, which is given by the width (FWHM) of the time dependent cluster potential energy curve. τ provides the time scale for the prevalence of the intracluster microscopic shock wave. The cluster size dependence of τ can be described in terms of a CSE, which can be traced to cluster

packing. The residence time obeys the relation[35]

$$\tau = R_c/v \quad , \tag{40}$$

where the cluster radius is given by Eq. (8), so that

$$[\tau(n)]^{-1} = (v/R_0)n^{-1/3} \quad . \tag{41}$$

This dynamic CSE is borne out by molecular dynamics simulations for high-energy collisions between neat inert-gas clusters and a metal surface (Fig. 5).[35] For a heterocluster containing a diatomic molecule embedded in an inert-gas cluster, whose cluster impact chemistry was explored by molecular dynamics simulations,[36] self volume corrections (section III.A) have to be introduced. This analysis[35,36] provided a quantification of dynamic cluster size effects.

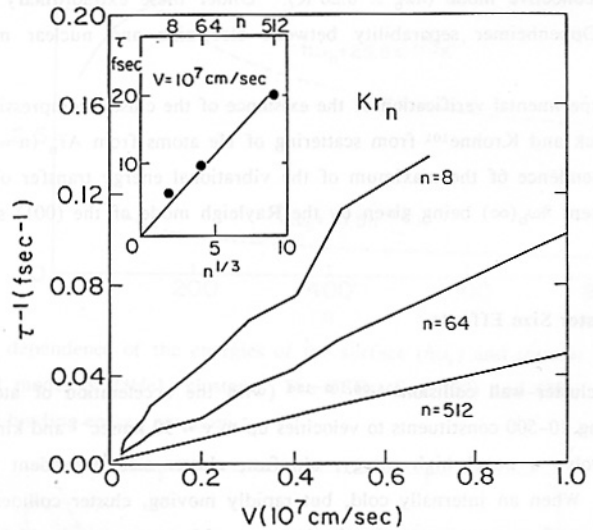

Fig. 5. The dependence of the inverse residence time of Kr_n clusters colliding with a Pt surface on the initial cluster velocity, according to Eq. (41). The insert shows the dependence of τ vs $n^{1/3}$ at a fixed cluster velocity $v = 10^7$ cmsec^{-1} (kinetic energy per particle of 43 eV). The CSE, Eq. (41), implies that $\tau = (R_0/v)n^{1/3}$, resulting in the reasonable value $R_0 = 2.2$ Å.

VII. Dimensionality Scaling of Cluster Size Equations

The preceding analysis of cluster size effects focused on the usual physical situation when both the finite cluster and the corresponding reference bulk material are three dimensional (D = 3). Cluster

chemical physics in low dimensionality[127] may be of interest, pertaining to the following physical situations.

(1) Lower geometrical cluster dimensionalities. These may involve finite "cluster wires" converging to an infinite wire (D = 1), or planar clusters converging to an infinite plane (D = 2) for supported "islands" on a substrate.

(2) Fractal clusters. These are characterized by a Hausdorf dimensionality[128] D, which satisfies two conditions:

(i) The correlation length for the (self similar) fractal structure is smaller than the cluster radius.

(ii) With increasing size the cluster converges to the macroscopic fractal structure.

Examples for fractal clusters involve clusters of porous materials.[127]

We shall consider dimensionality scaling of SCEs following the classification of section II.

(A) Dimensionality scaling due to cluster packing. The fraction of the surface atoms in a cluster of Hausdorf dimensionality D is $F = \bar{\alpha} n^{-1/D}$, where $\bar{\alpha}$ is a numerical constant. The energy per atom, Eq. (5), is replaced by $u(n) = u_v + \bar{\alpha}(u_s - u_v) n^{-1/D}$. The collective surface vibrational frequency is expected to be $\hbar\omega_s(n) \propto n^{-1/(D-1)}$, while the bulk compression mode is $\hbar\omega_b(n) \propto n^{-1/D}$. These heuristic relations constitute the generalization of the liquid drop model for D dimensions. A more careful examination of the dispersion relations for elementary excitations in fractal clusters[129] is still required.

(B) Dimensionality scaling of excluded volume effects. We consider now the situation when the cluster and the excluded volume are characterized by a common dimensionality, D (≠3). The extension of the CSEs just requires the replacements of the excluded volume corrections $C(R_c)$, Eq. (7), by integrations over a D dimensional space. The packing of the constituents is given by replacing Eq. (8) by $R_c \propto n^{1/D}$. The following results emerge:

(B1) Charging energy contribution. The excluded volume contribution for the ionization potentials is now $C_{(D)}(R_c) \propto \int_{R_c}^{\infty} d^D\vec{r}\, \vec{P}\cdot\vec{D}$, where $\vec{P}$ and $\vec{D}$ are the electric polarization and displacement vector, respectively, and the volume element is $d^D\vec{r} \propto r^{D-1}dr$. Accordingly, $C_{(D)}(R_c) \propto R_c^{D-4}$ and $C_{(D)}(n) \propto n^{(D-4)/D}$.

(B2) Spectroscopic observables. The excluded volume corrections in Eqs. (29), (31)-(34) in D dimensions are $C_{1,2}^{(D)}(R_c) \propto \int_{R_c}^{\infty} d^D\vec{r}\, \delta E(r)$, where $\delta E(r) = -e(r) \propto r^{-\mu}$ ($\mu = 6$) for the spectral shift and $\delta E(r) = [e(r)]^2 \propto r^{-2\mu}$ for the second moment. We immediately obtain for the excluded volume correction for the spectral shift $C_1^{(D)}(R_c) \propto R_c^{(D-\mu)}$ and for the excluded volume correction for the second spectral moment $C_2^{(\Delta)}(R_c) \propto R_c^{(D-2\mu)}$. For packing in D dimensions we obtain $C_1^{D}(n) \propto n^{(D-\mu)/D}$ and $C_2^{(D)}(n) \propto n^{(D-2\mu)/D}$. For the dispersive spectral shifts ($\mu = 6$) one obtains the appropriate excluded volume corrections for $\delta\nu(n)$ and $\Delta(n)$. The excluded volume corrections in conjunction with Eq. (7) result in the dimensionality scaling of the spectroscopic CSEs

$$\delta\nu(n) = \delta\nu(\infty) + An^{(D-6)/D} \tag{42}$$

$$\Delta(n) = \Delta(\infty) - Bn^{(D-12)/D} \quad , \tag{43}$$

where A and B are numerical constants.

These CSEs, originating from dimensionality scaling, may be of interest for the ionization and spectroscopic interrogation of doped clusters of lower dimensionality and of fractal clusters.

Acknowledgments

Thanks are due to Ori Cheshnovsky, Rina Giniger, Uzi Even, Israel Schek and Raphael D. Levine for most helpful discussions. This research was supported by the German-Israel Binational James Franck Program for laser-matter interaction.

References

(1) Friedel, J., J. Phys. (Paris), C2, 38, 1 (1977).
(2) Jortner, J., Ber. Bunsenges. Phys. Chem. 88, 188 (1984).
(3) Bjørnholm, S., Contemp. Phys. 31, 309 (1990).
(4) Proceedings of the International Meeting on Small Particles and Inorganic Clusters. J. Phys. (Paris), Colloque C 2, 38 (1977).
(5) Proceedings of the Second International Meeting on Small Particles and Inorganic Clusters, Lausanne. 1980. Surf. Sci. 106, 1-608 (1981).
(6) Proceedings of Bunsengesellschaft Discussion Meeting on Experiments on Clusters, Koningstein, 1983, Ber. Gunsenges. Phys. Chem. 88 (1984).
(7) Proceedings of the Third International Meeting on Small Particles and Inorganic Clusters, Berlin, 1985. Surf. Sci. 165, 1-1072 (1985).
(8) Träger, F. and Putlitz, G. zu (eds.), Metal Clusters. Proceedings of an International Symposium, Heidelberg; Springer: Berlin, Heidelberg, New York (1986).
(9) Jena, P., Rao, B. K., and Khanna, N., (eds.), The Physics and Chemistry of Small Clusters. NATO ASI Series; Plenum Press: New York (1986).
(10) Sugano, S., Nishima, Y., and Onishi, S. (eds.), Microclusters; Springer: Berlin, Heidelberg, New York (1987).
(11) Jortner, J., Pullman, A., and Pullman, B. (eds.), Large Finite Systems; Reidel: Dordrecht (1987).
(12) Benedek, G., Martin, T. P., and Pacchioni, G. (eds.), Elemental and Molecular Clusters; Springer: Berlin, Heidelberg, New York (1988).
(13) Scoles, G. (ed.), The Chemical Physics of Atomic and Molecular Clusters. Proceedings of the International School of Physics "Enrico Fermi", Course CVII; North Holland: Amsterdam (1990).
(14) Proceedings of the Fourth International Symposium on Small Particles and Inorganic Clusters, Aix en Provence, 1988, Z. Phys. D. - Atoms, Molecules and Clusters 12 (1989).
(15) Echt, O. and Recknagel, E. (eds.), Proceedings of the Fifth International Symposium on Small Particles and Inorganic Clusters, Konstanz, 1991, Z. Phys. D. - Atoms, Molecules and Clusters 19, 20 (1990).
(16) Sugano, S. Microcluster Physics; Springer Verlag: Berlin (1991).
(17) Berry, S. R., Burdett, J., and Castelman, A. W. (eds.), Small Particles and Inorganic Clusters, Z. Phys. D. - Atoms, Molecules and Clusters 26, 1 (1993).
(18) Jena, P., Khanna, S. N., and Rao, B. K. (eds.), Physics and Chemistry of Finite Systems: From Clusters to Crystals; Kluwer: Dordrecht (1992).
(19) Jortner, J. Z. Phys. D 24, 247 (1992).
(20) Jortner, J. and Ben-Horin, N. J. Chem. Phys. 98, 9346 (1993).
(21) Jortner, J. Zeitschr. für Physikalische Chemie 184, 283 (1994).
(22) Mackay, A. L., Acta Crystallogr. 15, 916 (1962).
(23) Hoare, M. R., Adv. Chem. Phys. 40, 49 (1969).
(24) Farges, J., De Feraudy, M. F., Raoult, B., and Torchet, G., J. Chem. Phys. 78, 5067 (1983).
(25) Farges, J., De Feraudy, M. F., Raoult, B., and Torchet, G., J. Chem. Phys. 84, 3491 (1986).
(26) Echt, O., Sattler, K., and Recknagel, E., Phys. Rev. Lett. 47, 1121 (1981).

(27) Echt, O., Kandler, O., Leisner, T., Miehle, W., and Recknagel, E. , Faraday Symposium No. 25 on Large Gas Phase Clusters (1989).
(28) Martin, T. P., Näher, U., Schaber, H., and Zimmermann, U., Phys. Rev. Lett. 70, 3079 (1993).
(29) Heer, W. de, Knight, W., Chou, M., and Cohen, M. L., Solid State Phys. 40, 93 (1986).
(30) Stringari, S., Phys. Lett. A 107, 36 (1985).
(31) Stringari, S. and Treiner, J., J. Chem. Phys. 87, 5021 (1987).
(32) Lewart, D. S., Pandharipande, V. T., and Pieper, S. R., Phys. Rev. 37, 4950 (1988).
(33) Fried, L. E. and Mukamel, S., Adv. Chem. Phys. 26, 217 (1993).
(34) Cheshnovsky, O., Giniger, R., Markovich, G., Makov, G., Nitzan, A., and Jortner, J. J. Chim. Phys. (this issue - in press).
(35) Even, U., Schek, I., and Jortner, J. Chem. Phys. Lett. 202, 303 (1993).
(36) Schek, I., Raz, T., Levine, R. D., and Jortner, J., J. Chem. Phys. (in press).
(37) Evans, R. D., The Atomic Nucleus; McGraw Hill: New York (1955).
(38) Bohr, A. and Mottelson, B. R., The Atomic Nucleus; W.A. Benjamin: New York (1969).
(39) Bréchignac, C., Cahuzac, Ph., Carlier, F., de Frutos, M., and Leygnier, J., Z. Phys. D 19, 1 (1991).
(40) Bréchignac, C., Cahuzac, Ph., Carlier, F., de Frutos, M., and Leygnier, J., J. Chem. Phys. 93, 7449 (1990).
(41) Arnold, G. H., Eaton, S. T., Sarkas, H. W., Bowen, K. H., Ludewight, C., and Haberland, H., Z. Phys D 20, 9 (1991).
(42) Markovich, G., Pollack, S., Giniger, R., and Cheshnovsky, O., Z. Phys. D 26, 98 (1993).
(43) Markovich, G., Giniger, R., and Cheshnovsky, O., J. Chem. Phys. (in press).
(44) Perera, L. and Berkowitz, M., J. Chem. Phys. 95, 1954 (1991).
(45) Perera, L. and Berkowitz, M., J. Chem. Phys. 99, 4222 (1993).
(46) Dang, L. X. and Garret, B. C., J. Chem. Phys. 99, 2972 (1993).
(47) Caldwell, J., Dang, L. X., and Kollman, P. A., J. Am. Chem. Soc., 112, 9144 (1990).
(48) Dang, L. X., Rice, J. E., Caldwell, J., and Kollman, P. A., J. Am. Chem. Soc. 113, 2481 (1991).
(49) Caldwell, J., Dang, L. X., and Kollman, P. A., J. Am. Chem. Soc. 112, 9145 (1990).
(50) Sung, S. and Jordan, P. C., J. Chem. Phys. 85, 4045 (1986).
(51) Dang, L. X. and Smith, D. E., J. Chem. Phys. 99, 6950 (1993).
(52) Combariza, J. E., Kestner, N. R., and Jortner, J., Chem. Phys. Lett. 203, 423 (1993).
(53) Combariza, J. E., Kestner, N. R., and Jortner, J., J. Chem. Phys. 100, 2851 (1994).
(54) Combariza, J. E. and Kesnter, N. R., J. Phys. Chem., 98, 3513 (1994).
(55) Combariza, J. E., Kestner, N. R., and Jortner, J., Chem. Phys. Lett., 221, 156 (1994).
(56) Möller, T., Z. Phys. D 20, 1 (1990).
(57) Wörmer, J. and Möller, T., Z. Phys. D 20, 39 (1991).
(58) Lengen, M., Joppien, M., Müller, R., Wörmer, J., and Möller, T., Phys. Rev. Lett., 68, 2362 (1992).
(59) Lengen, M., Joppien, M., von Pietorwski, R., and Möller, T., Chem. Phys. Lett. (in press).
(60) Goldberg, A., Heidenreich, A., and Jortner, J., J. Phys. Chem. (submitted).
(61) Böttcher, C. J. F., The Theory of Electric Polarization, 2nd Ed.; Elsevier: Amsterdam (1973).
(62) Brus, L. E., J. Chem. Phys. 79, 5566 (1983).
(63) Makov, G. and Nitzan, A., J. Phys. Chem. 98, 3459 (1994).
(64) Rips, I. and Jortner, J., J. Chem. Phys. 97, 536 (1992).
(65) Messing, I., Raz, B., and Jortner, J., Chem. Phys. 24, 183 (1977).
(66) Even, U., Amirav, A., Leutwyler, S., Ondrechen, M. O., Berkovitch-Yellin, Z., and Jortner, J., Faraday Discuss. Chem. Soc. 73, 153 (1982).
(67) Leutwyler, S. and Jortner, J., J. Phys. Chem. 91, 5558 (1987).
(68) Brumbaugh, D. V., Kenny, L. E., and Levy, D. H., J. Chem. Phys. 78, 3415 (1983).
(69) Stephenson, T. A. and Rice, S. A., J. Chem. Phys. 81, 1083 (1984).
(70) Alfano, J. C., Martinez, S. J., and Levy, D. H., Chem. Soc. Faraday Trans. 86, 2503 (1990).
(71) Heikal, A., Banares, L., Semmes, D. H., and Zewail, A. H., Chem. Phys. 156, 231 (1991).
(72) Leutwyler, S. and Bösiger, J., Chem. Rev. 90, 489 (1990).
(73) Amirav, A., Even, U., and Jortner, J., Chem. Phys. Lett. 67, 9 (1979).
(74) Amirav, A., Even, U., and Jortner, J., J. Chem. Phys. 75, 2489 (1981).
(75) Ben-Horin, N., Even, U., and Jortner, J., J. Chem. Phys. 97, 5988, 6011 (1992).
(76) Ben-Horin, N., Even, U., Jortner, J., and Leutwyler, S., J. Chem. Phys. 97, 5296 (1992).
(77) Heidenreich, A., Bahatt, D., Ben-Horin, N., Even, U., and Jortner, J., J. Chem. Phys. 100, 6290 (1994).

(78) Leutwyler, S. and Bösiger, J., Z. Phys. Chem. NF 154, 31 (1987).
(79) Bösiger, J. and Leutwyler, S., Phys. Rev. Lett. 59, 1895 (1987).
(80) Bösiger, J. and Leutwyler, S., in: Large Finite Systems; Jortner, J. and Pullman, B. (eds.); Reidel: Dordrecht, pp. 153-164 (1987).
(81) Leutwyler, S. and Bösiger, J., Faraday Discuss. Chem. Soc. 86, 225 (1988).
(82) Bösiger, J., Knochenmuss, R., and Leutwyler, S., Phys. Rev. Lett. 62, 3058 (1989).
(83) Knochenmuss, R. and Leutwyler, S., J. Chem. Phys. 92, 4686 (1990).
(84) Kelley, D. F. and Bernstein, E. R., J. Phys. Chem. 90, 5186 (1986).
(85) Nimlos, M. R., Young, M. R. and Bernstein, E. R., J. Phys. Chem. 91, 5286 (1989).
(86) Schmidt, M., Mons, M. and Le Calvé J., J. Phys. Chem. 96, 2402 (1992).
(87) Schmidt, M., Mons, M. and Le Calvé J., Chem. Phys. Lett. 177, 371 (1991).
(88) Schmidt, M., Mons, M., Le Calvé J., Millie, P., and Cossarg-Magos, C., Chem. Phys. Lett. 183, 69 (1991).
(89) Anderson, P.W. and Weiss, P. R., Rev. Mod. Phys. 25, 269 (1953).
(90) Kubo, R., Adv. Chem. Phys. 15, 101 (1969).
(91) Sue, J., Yan, Y. J., and Mukamel, S., J. Chem. Phys. 85, 462 (1986).
(92) Penner, A., Amirav, A., Jortner, J., and Nitzan, A., J. Chem. Phys. 93, 147 (1990).
(93) Crepin, C. and Tramer, A., Chem. Phys. Lett. 170, 446 (1990).
(94) Angelstaff, P. A., An Introduction to the Liquid State; Oxford University: Oxford (1990).
(95) Stringari, S., Z. Phys. D 20, 219 (1991).
(96) Stringari, S., in: The Chemical Physics of Atomic and Molecular Clusters, Scoles, G. (ed.), Proceedings of the International School of Physics "Enrico Fermi", 1988; North Holland: Amsterdam (1990).
(97) Jortner, J., Scharf, D., and Landman, U., in: Excited-State Spectroscopy in Solids, Grassano, V. and Terzi, N. (eds.), Proceedings of the International School of Physics "Enrico Fermi", Course XCVI, 1985; North Holland: Amsterdam (1987).
(98) Nabutovskii, V. M. and Romanov, D. A., Sov. J. Low Temp. 11, 277 (1985).
(99) Rama Krishna, M. V. and Whaley, K. B., Phys. Rev. B 38, 11839 (1985).
(100) Rosenblit, M. and Jortner, J., J. Chem. Phys. (in press).
(101) Buck, U. and Krohne, R., Phys. Rev. Lett. 73, 947 (1994).
(102) Beuhler, R. J. and Friedman, L., Intern. J. Mass Spectrom. Ion Phys. 23, 81 (1977).
(103) Friedman, L. and Vineyard, G. H., Comments At. Mol. Phys. 15, 251 (1977).
(104) Beuhler, R. and Friedman, L., Chem. Rev. 86, 521 (1986).
(105) Shapiro, M. H. and Tombrello, T. A., Phys. Rev. Lett. 65, 92 (1990).
(106) Shapiro, M. H. and Tombrello, T. A., Phys. Rev. Lett. 68, 1613 (1992).
(107) Mahoney, J. F., Perel, J., Lee, T. D., Martino, P. A., and Williams, P., J. Am. Soc. Mass Spectrom. 3, 311 (1992).
(108) Wolfgang, P. R. and Klingelhöfner, R., J. de Physique C 2, 159 (1989).
(109) Shulga, V. I., Nucl. Inst. Methods Phys. Res. B 58, 422 (1991).
(110) Hsieh, H., Averbach, R. S., Sellers, H., and Flynn, C. P., Phys. Rev. B 45, 4417 (1992).
(111) Haberland, H., Karraris, M., Mall, M., and Thurner, Y., J. Vac. Tech. A 10, 3266 (1992).
(112) Haberland, H., Insepov, Z., and Moseler, M., Z. Phys. D 26, 229 (1992).
(113) Yamada, I., Takaoka, G. H., Usui, H., and Koh, S. K., Mater. Res. Soc. Symp. Proc. 206, 383 (1991).
(114) Yamada, I., Appl. Surf. Sci. 43, 23 (1989).
(115) Yamamura, Y., Yamada, I., and Tagaki, T., Nucl. Instrum. Methods B 37/38, 902 (1987).
(116) Müller, K. H., J. App. Phys. 61, 2516 (1987).
(117) Cheng, H. P., and Landman, U., J. Phys. Chem. 98, 3527 (1994).
(118) St. John, P. M., Beck, R. D., and Whetten, R. L., Phys. Rev. Lett. 69, 1467 (1992).
(119) St. John, P. M. and Whetten, R. L., Chem. Phys. Lett. 196, 330 (1992).
(120) Beck, R. D., St. John, P. M., Alvarez, M. M., Diederich, F., and Whetten, R. L., J. Phys. Chem. 95, 8402 (1991).
(121) Yeretzian, C. and Whetten, R. L., Z. Phys. D 24, 199 (1992).
(122) Yeretzian, C., Hansen, K., and Whetten, R. L., Science 260, 652 (1993).
(123) Even, U., de Lange, P., Jonkman, H., and Kommandeur, J., Phys. Rev. Lett. 56, 956 (1986).
(124) Tögelhofer, K., Aumayr, F., Kunz, H., Winter, H., Scheier, P., and Märk, T. D., Europhys. Lett. 22, 597 (1993).
(125) Even, U., and Hendell, E. (to be published).
(126) Cleveland, C. L. and Landman, U., Science 257, 355 (1992).

(127) Fleischmann, M., Tildesley, D. J., and Ball, R. D. (eds.). Fractals in the Natural Sciences, Discussion Meeting Probs. Roy. Soc. (London) 423, 1, (1989).
(128) Mandelbrot, B. B., The Fractal Geometry of Nature; H. Freeman: New York (1982).
(129) Alexander, S. and Orbach, R., J. Phys. (Paris) 43, L625 (1983).